

# Pharmacophore Based Virtual Screening for Identification of Novel CDK<sub>2</sub> Inhibitors

Amar Issa<sup>1\*</sup>, Faten Sliman<sup>2</sup>, Jehad Harbali<sup>1</sup>

<sup>1</sup>Department of Pharmaceutical Chemistry and Quality Control, Faculty of Pharmacy, University of Damascus, Damascus, Syria

<sup>2</sup>Department of Pharmaceutical Chemistry and Quality Control, Faculty of Pharmacy, University of Tartous, Tartous, Syria

Email: \*amarissa28@hotmail.com

**How to cite this paper:** Issa, A., Sliman, F. and Harbali, J. (2021) Pharmacophore Based Virtual Screening for Identification of Novel CDK<sub>2</sub> Inhibitors. *International Journal of Organic Chemistry*, 11, 72-89.

<https://doi.org/10.4236/ijoc.2021.112007>

**Received:** April 26, 2021

**Accepted:** June 27, 2021

**Published:** June 30, 2021

Copyright © 2021 by author(s) and Scientific Research Publishing Inc.

This work is licensed under the Creative Commons Attribution International License (CC BY 4.0).

<http://creativecommons.org/licenses/by/4.0/>



Open Access

## Abstract

CDK<sub>2</sub> is one of the most important members of Cyclin-dependent kinases. It is a critical modulator of various oncogenic signaling pathways, and its activity is vital for loss of proliferative control during oncogenesis. This work has focused on developing a pharmacophore model for CDK<sub>2</sub> inhibitors by using a dataset of known inhibitors as a pre-filter throughout the virtual screening and docking process. Consequently, the best pharmacophore model was made of one hydrogen bond acceptor, and two aromatic ring features with a high correlation value of 0.906. The validation findings proved out that the selected model can be used as a filter to screen new molecules like Enamine kinase hinge region directed library against CDK<sub>2</sub>. As a result, 69 hits were subjected to molecular docking studies. Eventually, three compounds (5909, 701 and 8397) scored good interaction energy values and strong molecular interactions. Hence, they were identified as leads for novel CDK<sub>2</sub> inhibitors as anticancer drugs.

## Keywords

CDK<sub>2</sub>, Cancers, Docking, Inhibitors, Pharmacophore, Virtual Screening

## 1. Introduction

Cyclin-dependent kinases (CDKs) are members of the serine/threonine kinase family and they are key enzymes in cell-cycle progression and transcription. These kinases are dependent on cyclin-binding for their activation in order to play their biological roles. However, they were shown to be frequently deregulated in different human tumors. Consequently, CDKs have received increasing attention as targets for anticancer drugs [1] [2] [3]. One of the members of CDKs which play a crucial role in orchestrating cellular transit through the cell

cycle is CDK<sub>2</sub>. Therefore, CDK<sub>2</sub> is considered as an important target for new therapeutics designed to recover control of the cell cycle [4] [5] [6].

Nowadays, there is no doubt that new advances in computer-aided drug designing have reduced the effective cost and time involved in drug discovery. However, one of the most important and extensively used tools in drug discovery process is Pharmacophore modeling which employs compound collection to generate structural patterns that should be present in active compounds. These patterns represent the set of properties and their arrangement in 3D space that an active compound must possess for it [7]. Moreover, pharmacophore modelling has been routinely used in combination with other molecular modelling techniques. Once a pharmacophore model is generated, it can be used for querying the 3D chemical database to search for potential ligands, which is so-called “pharmacophore-based virtual screening” (VS) [8]. Consequently, it can be a useful filter to narrow down the number of compounds to be docked [9] [10].

As an example of a typical such use, Nicklaus *et al.* used a known inhibitor of HIV-1 integrase to build a high correlation pharmacophore model, search a database, and prioritize 267 possible leads. Sixty of those were tested, and 19 were found to inhibit the enzyme [11].

Furthermore, in terms of the urgency of developing high correlation pharmacophore models for CDK inhibitors using computer-aided methods, two different ligand-based pharmacophore models for CDK inhibitors have been independently reported depending on different selected training sets (**Figure 1**). Hecker's model was based on purine derivatives (activities against CDK1, CDK<sub>2</sub>) [12], Toba's was based on indenopyrazole scaffold (activities against cyclin E/CDK<sub>2</sub>) [13].

In this study, we aim to develop high correlation pharmacophore models for CDK<sub>2</sub> inhibitors by 3D QSAR pharmacophore generation module within discovery studio (Biovia, 2016, France) using ligands that belong to various classes of cyclin CDK<sub>2</sub> inhibitors. After validation with test set, prediction method and Fischer randomization method, the best pharmacophore model was used as a filter to search Enamine database for compounds with similar pharmacophore features. Database compounds with best fitness scores were then subjected to molecular docking. All in all, this work has used different tools in a synergistic way in order to discover new potential molecules as leads against CDK<sub>2</sub>.

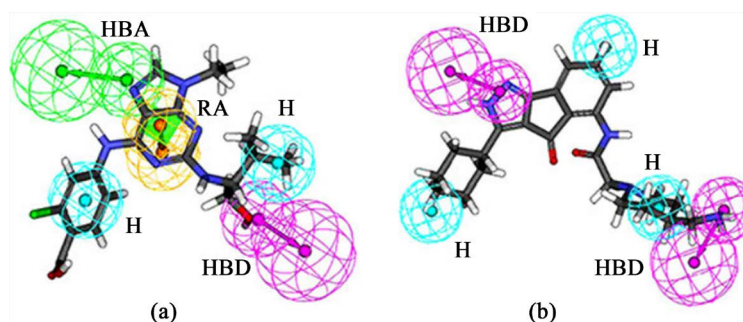


**Figure 1.** The ligand-based pharmacophore models of CDK<sub>2</sub> inhibitors reported previously by (a) Hecker *et al.* (b) Toba *et al.*

## 2. Materials and Methods

### 2.1. Protein Structure Preparation

A large number of crystal structures are available on human active and inactive CDK<sub>2</sub> in complex with small ligands which bind deeply within ATP site. However, protein complex with triazolopyrimidine inhibitor having the PDB code 2C6O and 2.1Å resolution was retrieved from the RCSB Protein Data Bank (PDB) to be used as a structural template [14].

Occasionally, the protein was prepared using general purpose protocol (Discovery Studio-Biovia 2016) by removing water molecules in all the system. Adding bond orders and formal charges to the hetero groups of the protein along with addition of hydrogens using charmM forcefield and finally minimizing energy using adopted basis Newton-Raphson algorithm (NR).

### 2.2. Pharmacophore Model Generation

#### 2.2.1. Selection of Training Set Compounds

3D Quantitative Structure-Activity Relationship (3D-QSAR) pharmacophore generation is designed to use HypoGen in order to produce predictive pharmacophores from a set of ligands with known activity values against a given biological target [15].

The structures of 51 CDK<sub>2</sub> inhibitors were obtained from literature [16]-[25] 16 diverse compounds (Figure 2) were selected for training data set basing on the principles of structural diversity and experimental activity values (IC<sub>50</sub>) spreading over four orders of magnitude (Table 1); Most active (IC<sub>50</sub> ≤ 15 nM,

**Table 1.** Training Set.

	Pdb Code	Ligand	IC50 (nM)	Structure
1	2A4L	R-roscovitine	400	Purine/Adenin Analogues
2	1G5S	H717	48	Purine/Adenin Analogues
3	1W0X	OLOMOUCINE	7	Purine/Adenin Analogues
4	1E1V	NU2058	17000	O6-Substituted Guanines
5	5D1J	BMs-387032/56H	48	Aminothiazole -based Inhibitors
6	2BHE	5-bromo Indirubin (BRY)	80	Oxindole-based Inhibitors
7	1E1X	NU6027 (NW1)	2200	Aminopyrimidine
8	1PXL	CK4	900	Aminopyrimidine
9	3S2P	PMU	68	Aminopyrimidine
10	2R3Q	5SC	1	Pyrazolopyrimidine
11	3WBL	PDY	23000	Pyrazolopyrimidine
12	2W05	FRT	1	Imidazolopyrimidine
13	1PXP	CK8	220	Thiopyrimidine
14	2VU3	AT7519	47	Pyrazolo based inhibitors
15	2VTQ	LZA	140	Pyazolo based inhibitors
16	2VV9	IM9	17	Triazole Based Inhibitors

++++), active ( $15 < IC_{50} \leq 200$  nM, +++), moderately active ( $200 < IC_{50} \leq 1000$  nM, ++), very low activity  $IC_{50} > 1000$  nM, +). Meanwhile, the remaining 35 molecules with known biological activities, served as the test set (Figure 3).

### 2.2.2. Generating and Validating 3d QSAR Pharmacophore Model

Pharmacophore prediction procedure according to HypoGen algorithm consists of three phases: a constructive, a subtractive, and an optimization phase. Occasionally, the idea of constructive phase is to generate pharmacophores that are common among the active molecules in the training set. In subtractive phase the program removes pharmacophores from the data structure that are not likely to be useful. The algorithm of optimization phase applies small perturbations to the pharmacophores created in the constructive and subtractive phases in an attempt to improve the score [17].

However, predictive pharmacophores are built by the HypoGen algorithm according to the selected data (training set of the sixteen selected molecules, 255 conformers for each compound were generated, only conformations within a 10 kcal/mol energy range were retained. In addition to that, Hydrogen bond acceptor (HBA), hydrogen bond donor (HBD), hydrophobic (HY), Hydrophobic aromatic (HA) and ring aromatic (RA) features were used to generate ten pharmacophore models, Uncertainty value was set to 3 and the minimum inter-feature distance was set to 1.5Å, all other parameters used in HypoGen module were kept at their default settings [26].

On the other hand, the generated pharmacophore models were then evaluated in order to choose the best one concerning; correlation coefficient, cost analysis and RMSD values. Furthermore, Fischer's randomization method was performed on the training set compounds in order to validate the statistical robustness of optimized model through verification of the correlation between the chemical structures and the biological activity [27]. In this validation process, the experimental activities of the training set used in HypoGen were scrambled randomly with the same parameters as those used for generating the original pharmacophore [28] [29]. A set of 19 random spreadsheets was generated with a confidence level of 95%.

Finally, the selected pharmacophore model was further validated by test set method using 35 molecules [30]. The test set validation method was carried out using not only ligand pharmacophore mapping protocol which identifies ligands that map to a pharmacophore, and aligns them to the query, but also ligand profiler protocol which maps a set of ligands against a set of pharmacophores.

### 2.3. Virtual Screening

The advantage of pharmacophore-based virtual screening in the drug discovery process is that most of the compounds with low probability to be active can be excluded early from further studies [31]. However, there are multiple pharmacophore-based virtual screening algorithms with the same principle: As an input, a small molecule database and a pharmacophore model are given, then each of

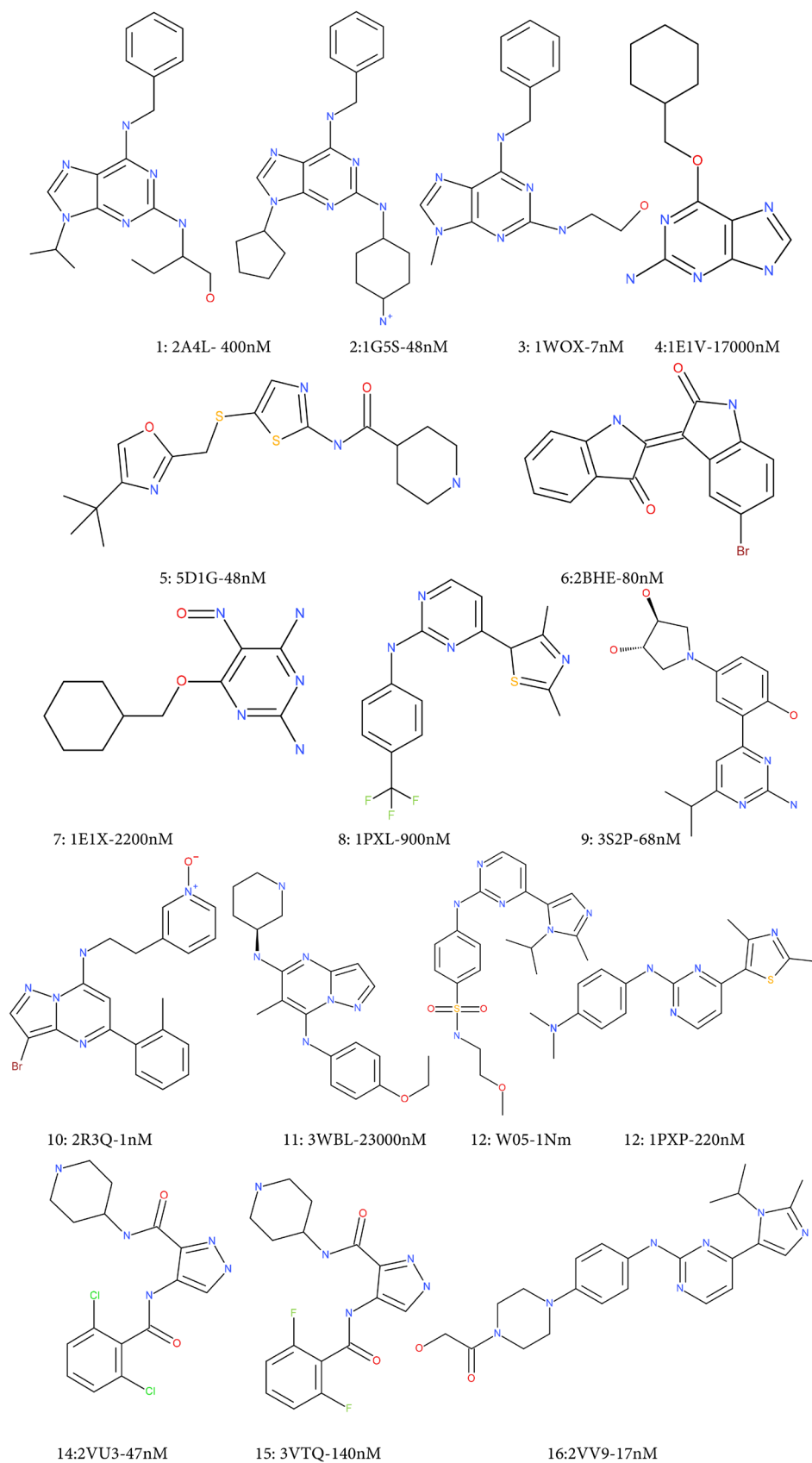
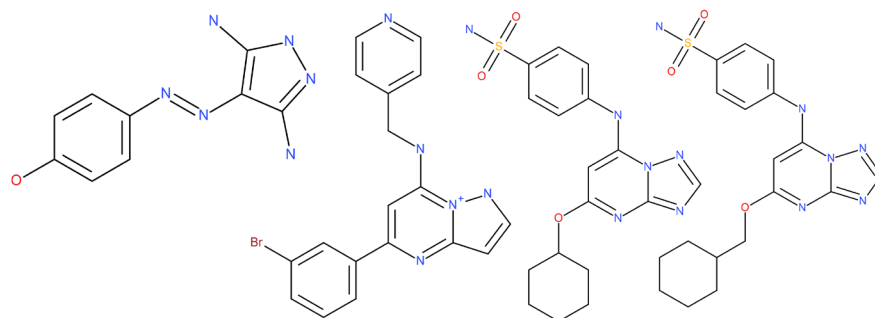


**Figure 2.** Training set.

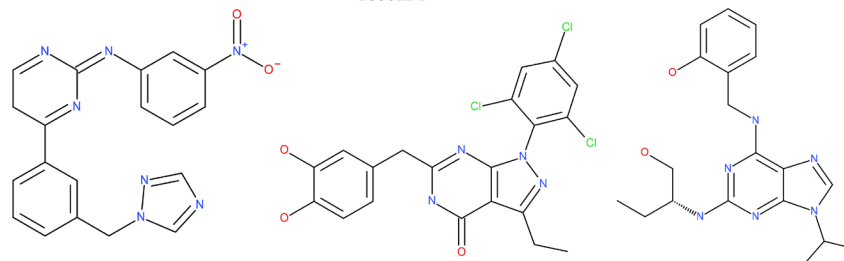


1: 2CLX  
2000nM

2: 2C68  
1800nM

3: 2C6M  
350nM

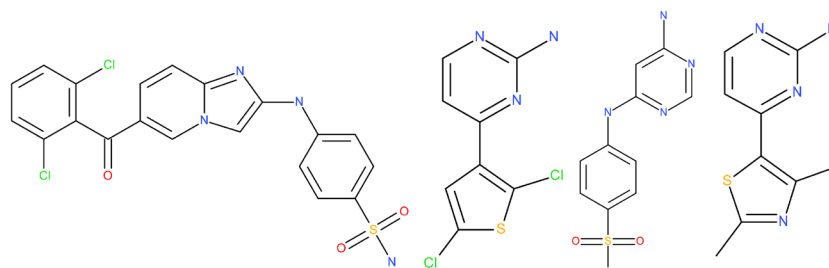
4: 2C6I  
11000nM



5: 2C5Y  
250nM

6: 2B54  
20nM

7: 2A0C  
55nM

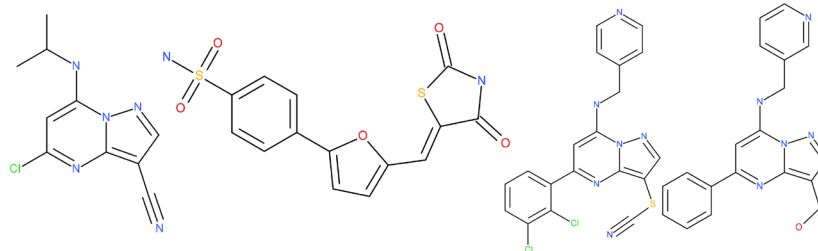


8: 1YKR  
560nM

9: 1PXI  
17000nM

10: 1JSV  
2000nM

11: 4FKL  
6500nM

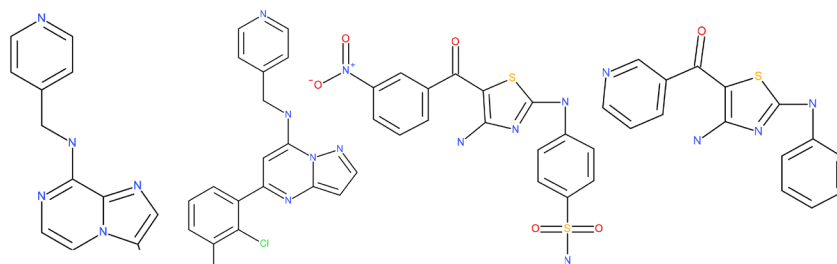


12: 2VTR  
1500nM

13: 2UZO  
27000nM

14: 2R3P  
900nM

15: 2R3O  
600nM



16: 2R3H  
20000nM

17: 2R3F  
500nM

18: 3QTX  
70nM

19: 3QTW  
650nM

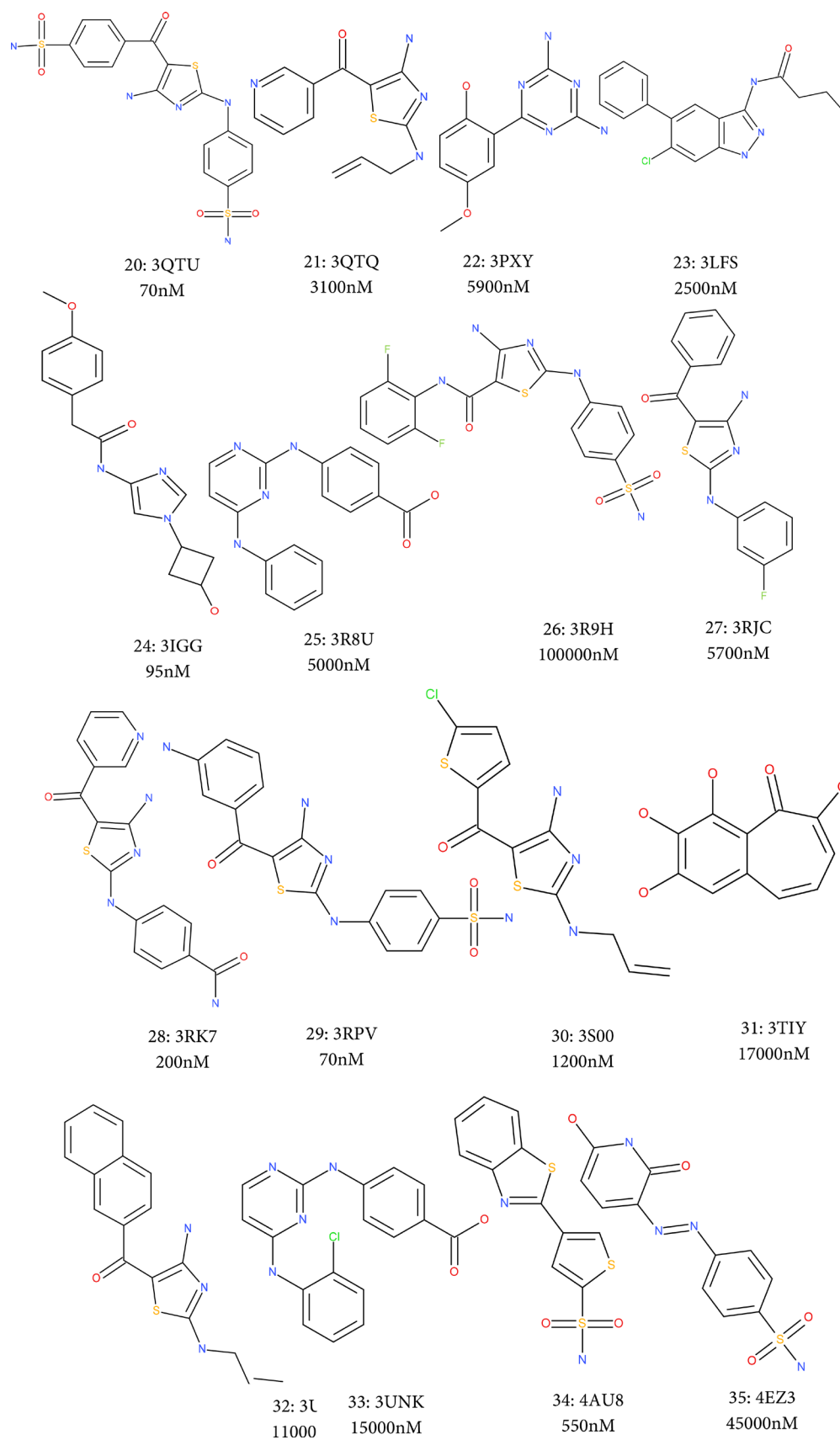


Figure 3. Test set.

the molecules conformations is fitted to the model. As result, a hit list, fitting compounds, are given as output [10].

Enamine Kinase-Hinge-Region-Directed-library which consists of 18,020 compounds was screened using Ligand Pharmacophore Mapping protocol and screen library protocol in order to search novel compounds which have the generated pharmacophore. Besides, retrieved compounds were filtered by applying Lipinski's rule of five (*i.e.*, a molecule with a molecular mass less than 500 Da, no more than 5 hydrogen bond donors, no more than 10 hydrogen bond acceptors, and an octanol-water partition coefficient  $\log P$  not greater than 5), and further sorted on the basis of fit value.

## 2.4. Docking

The selected compounds from Enamine library were docked into the active site of the previously prepared CDK<sub>2</sub> structure (2C60) with CDOCKER protocol implemented in Biovia Discovery Studio 2016. CDOCKER uses a CHARMM-based molecular dynamics (MD) scheme to dock ligands into a rigid receptor binding site. First, Random ligand conformations are generated using high-temperature MD. Second, the conformations are translated into the binding site. Third, Candidate poses are created using random rigid-body rotations followed by simulated annealing. A final minimization is then used to refine the ligand pose [32].

Moreover, the performance of the docking method on CDK inhibitors had been evaluated before it was carried out. The validation was achieved by measuring the RMSD between the orientation of the ligand existing in the crystal complex (2C6O) and its orientation found by our study. The RMSD value must be less than 2Å. However, CDOCKER interaction energy predicts the binding energies of the protein with retrieved hits [33]. The proximity between the receptor and hit was studied in terms of the electrostatic, hydrogen bond interactions and hydrophobic interaction.

## 3. Results and Discussion

### 3.1. Pharmacophore Modeling and Validation

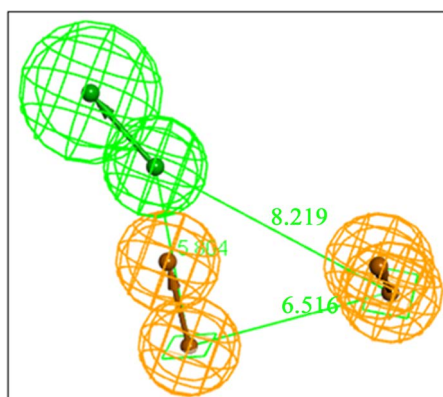
A set of ten pharmacophore models was generated based on a training set containing 16 structurally diverse compounds (Table 2).

In the present work, we will discuss the first pharmacophore model (Hypothesis 1) which is basically composed of three features: a hydrogen bond acceptor, and two aromatic ring features (Figure 4).

The first pharmacophore model was considered the best model for so many reasons. For instance, in terms of hypothesis significance, what really matters is the magnitude of the difference between the cost of any returned hypothesis and the cost of the null hypothesis. By the way, cost analysis shows a null cost value of 118.527 and Hypo1 cost value of 73.896. So, the cost difference for it was 44.631. A cost difference value above 40 implies that the pharmacophore model correlates the estimated and experimental activity values between (75% - 90%).

**Table 2.** Generated Pharmacophore Models.

Hypothesis	Correlation Factor	Total Cost	Features
1	0.906	73.896	HBA-Ring aromatic-Ring aromatic
2	0.889	75.499	HBA-Hydrophobic aromatic-Ring aromatic
3	0.883	75.788	HBA-Hydrophobic aromatic-Ring aromatic
4	0.880	76.123	HBA-Hydrophobic aromatic-Ring aromatic
5	0.880	76.312	HBA-HBA-Hydrophobic Aromatic
6	0.878	76.428	HBA-HBA-Hydrophobic Aromatic
7	0.865	77.654	HBA-Ring Aromatic-Ring aromatic
8	0.865	77.659	HBA-HBA-Hydrophobic Aromatic
9	0.863	78.055	HBD-Hydrophobic aromatic-Ring aromatic
10	0.86	78.080	HBA-Hydrophobic aromatic-Ring aromatic

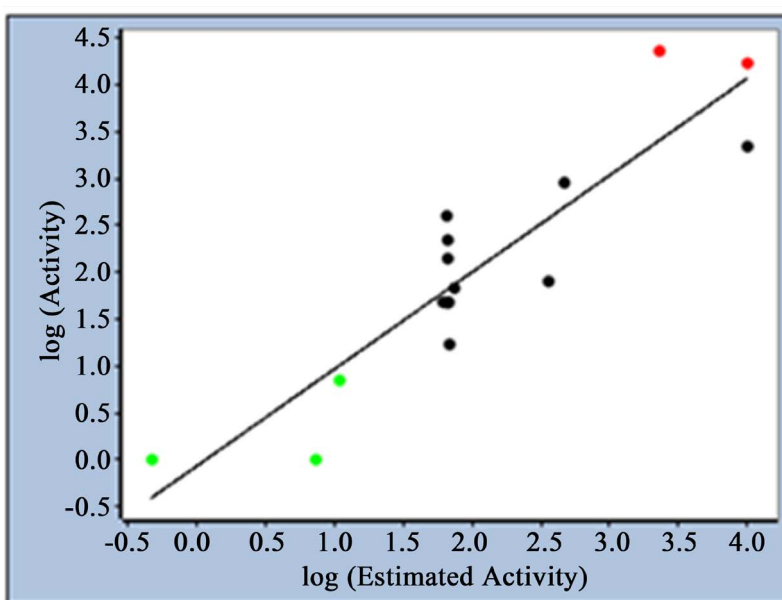
**Figure 4.** Pharmacophore Model (Hypo1).

Besides, total cost value should be away from the null cost and close to the fixed cost. However, among the total cost values of ten pharmacophore models, Hypo1 scored the closest value to the fixed cost value (63.187) than other models. Therefore, Hypo1 could be considered as a good model. In addition to the cost analysis of the models, hypothesis 1 was further assessed based on many factors. First, the correlation value of the first pharmacophore model was 0.906. Second, estimated activities of all ligands, even the lowest active one, were within one order of magnitude of the actual activity (**Table 3**). Hence, it is considered as an acceptable prediction of activity. The predictive ability of Hypo 1 on training set compounds is shown in **Figure 5**.

Third, the alignment of the training set ligands to the pharmacophore was taken into consideration in terms of its ability to explain the activity of the ligands. For instance, active ligands should map more features than inactive ligands. In other words, a ligand is inactive because it does not have an important feature, or the feature is present but cannot be oriented correctly in space. Occasionally, a general guideline for evaluating 3D QSAR pharmacophores is that the two most active ligands should map to all features of the pharmacophore.

**Table 3.** Training set aligned to the highest ranked Pharmacophore (hypo1).

Name	Fit	Est	Act	Mapping
2W05	5.3600	7.4000	1	[18,8,20]
2R3Q	6.5500	0.48000	1	[26,11,1]
1W0X	5.2000	11	7	[14,17,1]
2VV9	4.4000	69	17	[31,*,16]
2VU3	4.4100	67	47	[*,15,7]
1G5S	4.4400	62	48	[*,3,13]
5D1J	4.4000	68	48	[*,10,2]
3S2P	4.3600	75	68	[7,*,17]
2BHE	3.6800	360	80	[*,13,1]
2VTQ	4.4100	67	140	[*,15,7]
1PXP	4.4000	67	220	[9,*,15]
2A4L	4.4100	66	400	[1,*,21]
1PXL	3.5600	470	900	[19,5,*]
1E1X	2.2300	10,000	2200	[*,1,*]
1E1V	2.2300	10,000	17,000	[*,1,*]
3WBL	2.8700	2300	23,000	[*,12,19]

**Figure 5.** The correlation graph between experimental and estimated activity values based on hypo1.

**Table 3** summarizes the training set aligned to the first pharmacophore model and illustrates that the three most active ligands have mapped to all features of the pharmacophore. **Figure 6** illustrates the most active compound (2R3Q) mapped to the features of hypo1.

Forth, the result of Fischer's randomization test confirmed the statistical confidence of Hypo1 and indicated that none of the randomly generated pharmacophore models obtained from this validation method scored better statistical values than Hypo1.

Finally, a test set of 35 ligands with known biological activity was used in order to determine the best models by assessing their ability to estimate the activity of a test set. Consequently, 24 compounds were mapped to the proposed pharmacophore (Table 4), the other 11 compounds which have not been mapped had activities over 1000 nm. Figure 7 represents the most active ligand of test set (2A0C) mapped to hypo1.

Thus, the hypothesis 1 is considered to be a good model to estimate the activity of new compounds. Moreover, heat map plot maps test set ligands to the set of generated pharmacophores by 3D QSAR. It represents fit values in a two-dimensional color map. As they are shown in (Figure 8), blue rectangles

**Table 4.** Mapped molecules of test set with hypo1.

Index	Name	Ic50 (nm)	Fit value	Index	Name	Ic50 (nm)	Fit value
1	2A0C	55	5.74741	13	4AU8	551	3.21273
2	2R3P	900	5.70553	14	3IGG	95	2.88812
3	3UNJ	11,000	5.58545	15	3RK7	200	2.68082
4	2R3F	500	5.52399	16	3R9H	100,000	2.66294
5	3UNK	15,000	5.45168	17	2C6M	350	2.65442
6	2C68	1800	5.44727	18	2C6I	11,000	2.54907
7	2R3O	600	4.88627	19	1YKR	560	1.70494
8	2B54	20	4.67484	20	3QTW	650	1.64192
9	2C5Y	150	4.50005	21	3RJC	5700	1.59893
10	3RPV	70	4.45479	22	1JSV	2000	1.38688
11	3QTX	70	4.03065	23	3LFS	2500	0.753145
12	3QTU	70	3.66091	24	2UZO	27,000	0.457822

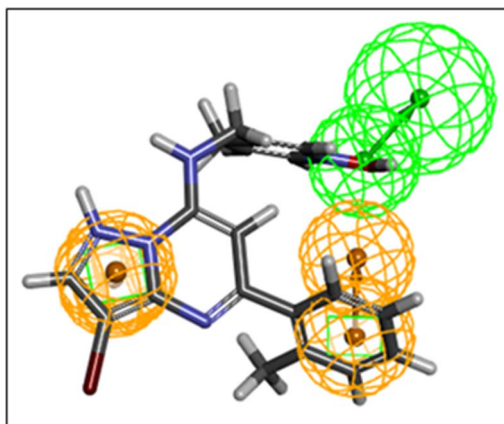


**Figure 6.** 2R3Q mapped to hypo 1.

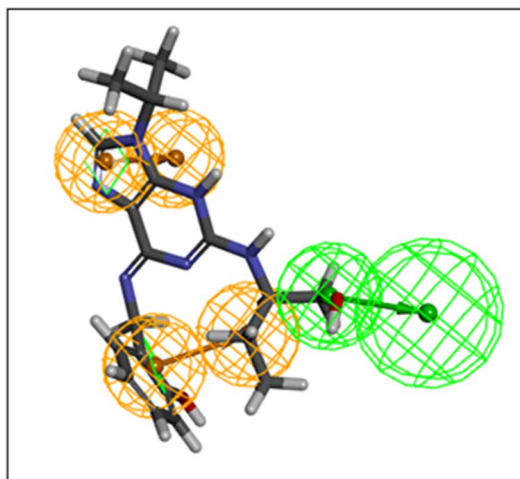


Figure 7. 2A0C mapped to the hypo1.

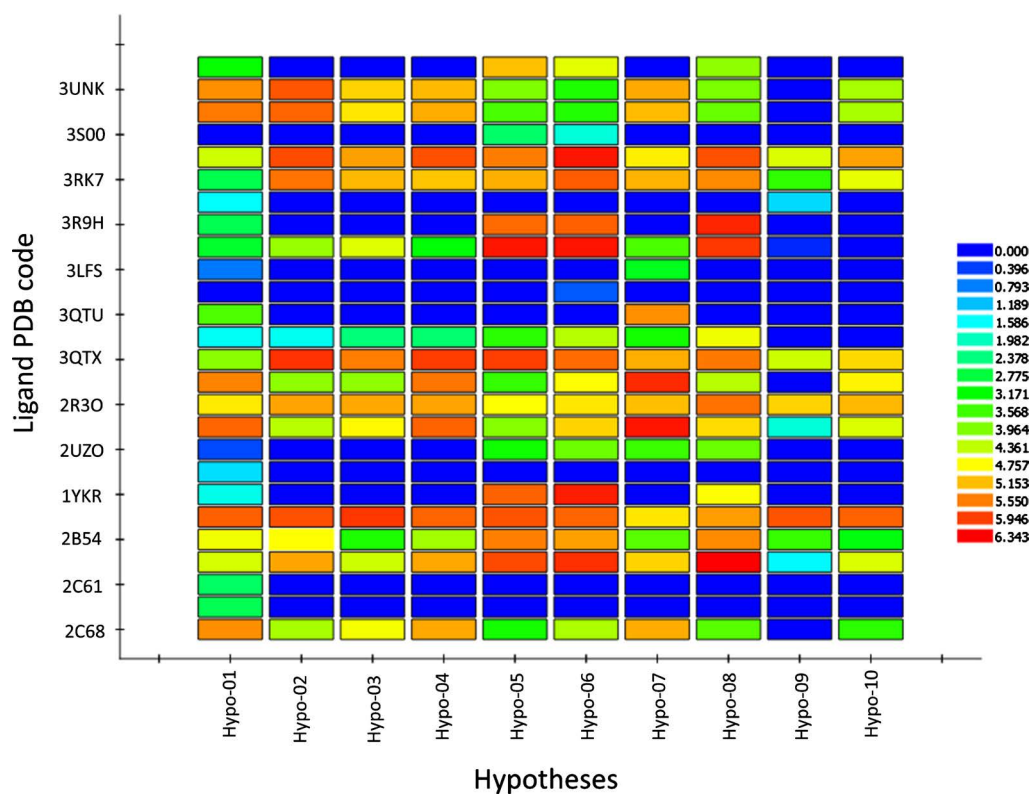


Figure 8. Heat map plot of test set with pharmacophore models.

which simulate low fit values are less in hypo 1 than the other nine hypotheses, which indicates beside the other statistical validation indicators that virtual screening can be carried out basing on hypo 1.

### 3.2. Virtual Screening

There is no doubt that pharmacophore models are excellent tools for scaffold hopping and identifying structurally diverse compounds as hits by using them as a filter in virtual screening. Eventually, the validated pharmacophore model

(hypothesis1) has been used as 3Dimensional structural query to screen Enamine Kinase-Hinge-Region-Directed-Library of 18,020 compounds which has been also gone under Lipinski filtration in order to evaluate their druglikeness and determine if they have chemical and physical properties that would make it a likely orally active drug in humans.

However, when a compound from the database will be considered as a hit, two criterions are employed, it needs to match to all of the pharmacophore features and to have high fit value. In other words, since the Fit Value is based on the actual distances of the conformation from the pharmacophore feature centers, the better fit gives a higher score and directly describes how well the compound fits to the model. As a result, 69 hits were retrieved according to the Fit values over 5.8 and to the Lipinski filtration results.

### 3.3. Molecular Docking

The crystal structure of CDK<sub>2</sub> from the protein data bank (PDB ID: 2C6O) was selected and prepared for docking studies. Besides, the performance of the docking method on CDK inhibitors was evaluated by re-docking crystal ligand with less than 2 RMSD value. 69 hits with the highest fit value (over 5.8) were docked into the active site of CDK<sub>2</sub> using CDocker. As a result, compound 5909 (**Figure 9(a)**), compound 701 (**Figure 9(b)**) and compound 8397 (**Figure 9(c)**) showed very good binding modes with -CDocker interaction energy of 54.519, 52.665 and 48.94, respectively.

However, compound 5909 formed many significant interactions with the key binding amino acid residues of CDK<sub>2</sub> (**Figure 10(a)**). For instance, N atom

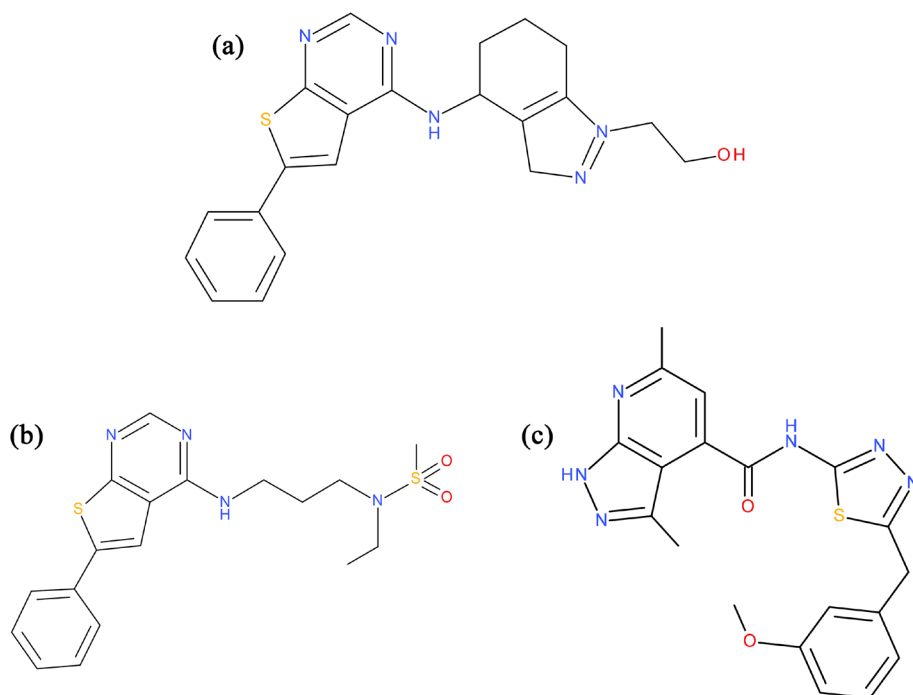


**Figure 9.** Hit compounds (a) compound 5909; (b) compound 701; (c) compound 8397.

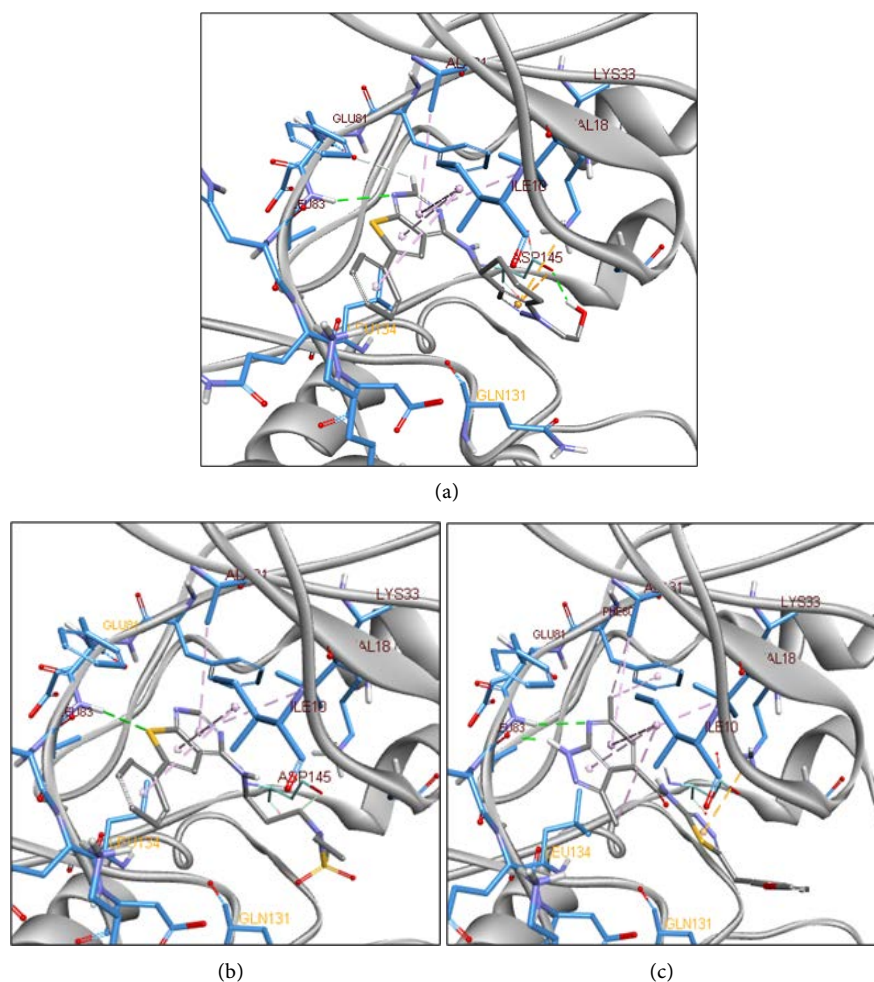


**Figure 10.** Interaction of HTS hit compounds with CDK<sub>2</sub>: The result of docking study of CDK<sub>2</sub> with (a) is hit 5909; (b) indicates hit 701; (c) shows 8397. The residues in the hinge-region ATP site are shown in blue. Schematic representation of hydrogen bonding (greenish dotted lines) and electrostatic interactions (pi-cation and pi-anion) in dotted orange lines, hydrophobic Pi-alkyl in dotted purple lines.

(which functions as a Hydrogen bond acceptor) in pyrimidine ring showed a hydrogen bond reaction with LEU83 (particularly with NH), as well as H atom (HBA) which is located between the two Nitrogens of pyrimidine ring interacted with the carbonyl group (HBD) of GLU81 by a hydrogen bond reaction. H atom in the side chain formed a hydrogen bond with ASP145 which is located in ribose region of ATP and which also interacted with the centroid of Pi ring of imidazole by a Pi-anion interaction. Besides, a Pi-cation interaction was formed between the electrons of a delocalized Pi system of imidazole in the side chain of the molecule and the positively charged Nitrogen in LYS33 side chain (in triphosphate region of ATP). Finally, pyrimidine ring formed a hydrophobic Pi-alkyl interaction bond with each of VAL18, ALA31 and ILE10. Meanwhile, ILE10 also interacted with each of thiophene ring and phenyl ring by a Pi-alkyl bond.

701 is also one of the compounds which were marked as hits (**Figure 10(b)**). Occasionally, S atom in thiophen ring showed a hydrogen bond reaction with

NH of LEU83. Another hydrogen bond was formed between the side chain and ASP145. Furthermore, there were hydrophobic Pi-alkyl interaction bonds between pyrimidine ring and each of VAL18 and ALA31, and between each of thiophene rings, and phenyl ring with ILE10.

The third hit in our study was compound 8397 (**Figure 10(c)**): Each of N atom (which functions as an HBD) in pyridine ring and NH (HBA) in pyrazole ring showed a hydrogen bond reaction with LEU83 (with NH and carbonyl group, respectively). Thiadiazole ring in the side chain of the compound interacted with Lys33 by an electrostatic Pi-cation bond. Besides, hydrophobic Pi-alkyl interaction bonds were formed by pyridine ring with each of VAL18, ALA31 and ILE10, pyrazole ring with IL10, and methyl group which is substituted on pyridine with PHE80. Moreover, substituted methyl groups on pyridine and pyrazole showed hydrophobic alkyl bonds with each of ALA31 and IL10, respectively.

All in All, binding modes and cdocker interaction energy values of compounds 5909, 701 and 8397 suggest them as good leads in order to design novel CDK<sub>2</sub> inhibitors.

#### 4. Conclusions

In the present work, a highly correlating ( $r = 0.906$ ) pharmacophore model (hypo1) containing one hydrogen bond acceptor, and two aromatic ring features was developed according to a group of compounds with known activity values (training set). In addition to its correlation factor, the generated pharmacophore approved to have a strong significance due to its good statistical values like total cost, fit values, RMSD. On the other hand, the model was further validated by a test set prediction method and Fischer randomization method.

However, this validated pharmacophore model was used for database screening (Enamine kinase hinge region directed library) in order to identify compounds which can be used in developing potent CDK<sub>2</sub> inhibitors as proposed anti-cancer drugs. Furthermore, molecular docking study which was carried out for the 69 retrieved hits from the virtual screening study showed that the CDOCKER interaction energy values of the compounds 5909, 701 and 8397 of Enamine library and their ability to form bond interactions with the key binding elements of the protein (LEU83, GLU81, ASP145, LYS 33, IL10) suggest these compounds to be good probable leads against CDK<sub>2</sub>.

#### Conflicts of Interest

The authors declare no conflicts of interest regarding the publication of this paper.

#### References

- [1] Cicen, J., Kalyan, K., Sorokinas, A., et al. (2014) Highlights of the Latest Advances in Research on CDK Inhibitors. *Cancers (Basel)*, **6**, 2224-2242.

- <https://doi.org/10.3390/cancers6042224>
- [2] Cicenás, J. and Valius, M. (2011) The CDK Inhibitors in Cancer Research and Therapy. *Journal of Cancer Research and Clinical Oncology*, **137**, 1409-1418. <https://doi.org/10.1007/s00432-011-1039-4>
- [3] Matthews, D.J. and Gerritsen, M.E. (2008) Targeting Protein Kinases for Cancer Therapy.
- [4] Schonbrunn, E., Betzi, S., Alam, R., *et al.* (2013) Development of Highly Potent and Selective Diaminotiazole Inhibitors of Cyclin-Dependent Kinases. *Journal of Medicinal Chemistry*, **56**, 3768-3782. <https://doi.org/10.1021/jm301234k>
- [5] Sánchez-Martínez, C., Lallena, M.J., Sanfeliciano, S.G. and de Dios, A. (2019) Cyclin Dependent Kinase (CDK) Inhibitors as Anticancer Drugs: Recent Advances (2015-2019). *Bioorganic and Medicinal Chemistry Letters*, **29**, Article ID: 126637. <https://doi.org/10.1016/j.bmcl.2019.126637>
- [6] Li, Y., Zhang, J., Gao, W., *et al.* (2015) Insights on Structural Characteristics and Ligand Binding Mechanisms of CDK<sub>2</sub>. *International Journal of Molecular Sciences*, **16**, 9314-9340. <https://doi.org/10.3390/ijms16059314>
- [7] Oranit Dror, A.S.-P., Nussinov, R. and Wolfson, H.J. (2006) Predicting Molecular Interactions *in Silico*. I. An Updated Guide to Pharmacophore Identification and Its Applications to Drug Design. *Frontiers in Medicinal Chemistry*, **3**, 551-584. <https://doi.org/10.2174/978160805206610603010551>
- [8] Ferreira, L., dos Santos, R., Oliva, G. and Andricopulo, A. (2015) Molecular Docking and Structure-Based Drug Design Strategies. *Molecules*, **20**, 13384-13421. <https://doi.org/10.3390/molecules200713384>
- [9] Caporuscio, F. and Tafi, A. (2011) Pharmacophore Modelling: A Forty Year Old Approach and Its Modern Synergies. *Current Medicinal Chemistry*, **18**, 2543-2553. <https://doi.org/10.2174/092986711795933669>
- [10] Vuorinen, A. and Schuster, D. (2015) Methods for Generating and Applying Pharmacophore Models as Virtual Screening Filters and for Bioactivity Profiling. *Methods*, **71**, 113-134. <https://doi.org/10.1016/j.ymeth.2014.10.013>
- [11] Yves Pommier, C.M. and Neamati, N. (2000) Retroviral Integrase Inhibitors Year 2000: Update and Perspectives. *Antiviral Research*, **47**, 139-148. [https://doi.org/10.1016/S0166-3542\(00\)00112-1](https://doi.org/10.1016/S0166-3542(00)00112-1)
- [12] Hecker, E., Andrea, T., *et al.* (2002) Use of Catalyst Pharmacophore Models for Screening of Large Combinatorial Libraries. *The Journal for Chemical Information and Computer Scientists*, **42**, 1204-1211. <https://doi.org/10.1021/ci020368a>
- [13] Toba, S., Maynard, A.J. and Sutter, J. (2006) Using Pharmacophore Models to Gain Insight into Structural Binding and Virtual Screening: An Application Study with CDK<sub>2</sub> and Human DHFR. *Journal of Chemical Information and Modeling*, **46**, 728-735. <https://doi.org/10.1021/ci050410c>
- [14] Richardson, C.M., Williamson, D.S., Parratt, M.J., *et al.* (2006) Triazolo[1,5-a]pyrimidines as Novel CDK<sub>2</sub> Inhibitors: Protein Structure-Guided Design and SAR. *Bioorganic and Medicinal Chemistry Letters*, **16**, 1353-1357. <https://doi.org/10.1016/j.bmcl.2005.11.048>
- [15] Lin, S.-K. (2000) Pharmacophore Perception, Development and Use in Drug Design. Edited by Osman F. Güner. *Molecules*, **5**, 987-989. <https://doi.org/10.3390/50700987>
- [16] Chohan, T., Qian, H., Pan, Y. and Chen, J.-Z. (2014) Cyclin-Dependent Kinase-2 as a Target for Cancer Therapy: Progress in the Development of CDK<sub>2</sub> Inhibitors as

- Anti-Cancer Agents. *Current Medicinal Chemistry*, **22**, 237-263.  
<https://doi.org/10.2174/0929867321666141106113633>
- [17] De Azevedo Jr., W.F. and Kim, S.H. (1997) Inhibition of Cyclin-Dependent Kinases by Purine Analogues: Crystal Structure of Human CDK<sub>2</sub> Complexed with Roscovitine. *European Journal of Biochemistry*, **526**, 518-526.  
<https://doi.org/10.1111/j.1432-1033.1997.0518a.x>
- [18] Jones, C.D., Andrews, D.M., Barker, A.J., et al. (2008) Imidazole Pyrimidine Amides as Potent, Orally Bioavailable Cyclin-Dependent Kinase Inhibitors. *Bioorganic & Medicinal Chemistry Letters*, **18**, 6486-6489.  
<https://doi.org/10.1016/j.bmcl.2008.10.075>
- [19] Harrison, L.R., Ottley, C.J., Pearson, D.G., et al. (2009) The Kinase Inhibitor O6-Cyclohexylmethylguanine (NU2058) Potentiates the Cytotoxicity of Cisplatin by Mechanisms That Are Independent of Its Effect upon CDK<sub>2</sub>. *Biochemical Pharmacology*, **77**, 1586-1592. <https://doi.org/10.1016/j.bcp.2009.02.018>
- [20] Dreyer, M.K., Borcherdig, D.R., Dumont, J.A., et al. (2001) Crystal Structure of Human Cyclin-Dependent Kinase 2 in Complex with the Adenine-Derived Inhibitor H717. *Journal of Medicinal Chemistry*, **44**, 524-530.  
<https://doi.org/10.1021/jm001043t>
- [21] Schulze-gahmen, U., Brandsen, J., Jones, H.D., Morgan, D., Meijer, L. and Ve, J. (1995) Multiple Modes of Ligand Recognition: Crystal Structures of Cyclin-Dependent Protein Kinase 2 in Complex with ATP and Two Inhibitors, Olomoucine and Isopen-tenyladenine. *Proteins: Structure, Function, and Bioinformatics*, **22**, 378-391.  
<https://doi.org/10.1002/prot.340220408>
- [22] Misra, R.N., Xiao, H.Y., Kim, K.S., Lu, S., Han, W.C., Barbosa, S.A., Hunt, J.T., Rawlins, D.B., Shan, W., Ahmed, S.Z., Qian, L., Chen, B.C., Zhao, R., Bednarz, M.S., Kellar, K.A., Mulheron, J.G., Batorsky, R., Roongta, U., Kamath, A., Kimball, S.D., et al. (2004) N-(Cycloalkylamino)acyl-2-aminothiazole Inhibitors of Cyclin-Dependent Kinase 2. N-[5-[[[5-(1,1-Dimethylethyl)-2-oxazolyl]methyl]thio]-2-thiazolyl]-4-piperidinecarboxamide (BMS-387032), a Highly Efficacious and Selective Antitumor Agent. *Journal of Medicinal Chemistry*, **47**, 1719-1728.  
<https://doi.org/10.1021/jm0305568>
- [23] Arris, C.E., Boyle, F.T., Calvert, A.H., et al. (2000) Identification of Novel Purine and Pyrimidine Cyclin-Dependent Kinase Inhibitors with Distinct Molecular Interactions and Tumor Cell Growth Inhibition Profiles. *Journal of Medicinal Chemistry*, **43**, 2797-2804. <https://doi.org/10.1021/jm990628o>
- [24] Finlay, M.R.V., Acton, D.G., Andrews, D.M., et al. (2008) Imidazole Piperazines: SAR and Development of a Potent Class of Cyclin-Dependent Kinase Inhibitors with a Novel Binding Mode. *Bioorganic & Medicinal Chemistry Letters*, **18**, 4442-4446.  
<https://doi.org/10.1016/j.bmcl.2008.06.027>
- [25] Eisenbrand, G., Hippe, Æ.F. and Jakobs, Æ.S. (2004) Molecular Mechanisms of Iridubin and Its Derivatives: Novel Anticancer Molecules with Their Origin in Traditional Chinese Phytomedicine. *Journal of Cancer Research and Clinical Oncology*, **130**, 627-635. <https://doi.org/10.1007/s00432-004-0579-2>
- [26] Brogi, S., Kladi, M., Vagias, C., Papazafiri, P., Roussis, V. and Tafi, A. (2009) Pharmacophore Modeling for Qualitative Prediction of Antiestrogenic Activity. *Journal of Chemical Information and Modeling*, **49**, 2489-2497.  
<https://doi.org/10.1021/ci900254b>
- [27] P, S.K., Singh, A. and Sharma, S. (2015) Ligand Based Pharmacophore Modeling, Virtual Screening and Molecular Docking for Identification of Novel CYP51 Inhi-

- bitors. Abstract Dataset Collection. *ChemInform*, **1**, 2.
- [28] Ramachandran, V., Padmanaban, E. and Ponnusamy, K. (2016) RSC Advances Pharmacophore Based Virtual Screening for Identification of Marine Bioactive Compounds as Inhibitors against Macrophage Infectivity Potentiator (Mip) Protein of *Chlamydia trachomatis*. *RSC Advances*, **6**, 18946-18957. <https://doi.org/10.1039/C5RA24999F>
- [29] Niu, M., Dong, F., Tang, S., et al. (2013) Pharmacophore Modeling and Virtual Screening for the Discovery of New Type 4 cAMP Phosphodiesterase (PDE4) Inhibitors. *PLoS ONE*, **8**, e82360. <https://doi.org/10.1371/journal.pone.0082360>
- [30] Vazquez, J., Lopez, M., Gibert, E., Herrero, E. and Luque, F.J. (2020) Merging Ligand-Based and Structure-Based Methods in Drug Discovery: An Overview of Combined Virtual Screening Approaches. *Molecules*, **25**, 4723. <https://doi.org/10.3390/molecules25204723>
- [31] Wu, G., Robertson, D.H., Iii, C.L.B. and Vieth, M. (2003) Detailed Analysis of Grid-Based Molecular Docking: A Case Study of CDOCKER—A CHARMM-Based MD Docking Algorithm. *Journal of Computational Chemistry*, **24**, 1549-1562. <https://doi.org/10.1002/jcc.10306>
- [32] Kaserer, T., Beck, K.R., Akram, M., Odermatt, A. and Schuster, D. (2015) Pharmacophore Models and Pharmacophore-Based Virtual Screening: Concepts and Applications Exemplified on Hydroxysteroid Dehydrogenases. *Molecules*, **20**, 22799-22832. <https://doi.org/10.3390/molecules201219880>
- [33] Singh, A.K., Raj, V. and Saha, S. (2017) Indole-Fused Azepines and Analogues as Anticancer Lead Molecules: Privileged Findings and Future Directions. *European Journal of Medicinal Chemistry*, **142**, 244-265. <https://doi.org/10.1016/j.ejmech.2017.07.042>